Journal of Volcanology and Geothermal Research 327 (2016) 469–483

Contents lists available at ScienceDirect

Journal of Volcanology and Geothermal Research

journal homepage: www.elsevier.com/locate/jvolgeores

The influence of effusion rate and rheology on lava flow dynamics and morphology: A case study from the 1971 and 1988–1990 eruptions at Villarrica and Lonquimay volcanoes, Southern Andes of Chile

Angelo Castruccio *, María Angélica Contreras

Departamento de Geología, Universidad de Chile, Plaza Ercilla 803, Casilla 13518, Santiago, Chile
Centro de Excelencia en Geotermia de los Andes (CEGA), Chile

ARTICLE INFO

Article history:
Received 16 February 2016
Received in revised form 5 August 2016
Accepted 20 September 2016
Available online 22 September 2016

Keywords:
Lava flows
Lonquimay volcano
Villarrica volcano
Effusion rate
Rheology

ABSTRACT

We analyzed two historical lava flows from the Southern Andes of Chile: The lava flows from the 1971 Villarrica volcano eruption and the 1988–1990 Lonquimay volcano eruption. The 1971 lava flow has a volume of 2.3×10^7 m^3, a maximum length of 16.5 km and was emplaced in two days, with maximum effusion rates of ~800 m^3/s. The lava has a mean width of 150 m and thicknesses that decrease from 10 to 12 m at 5 km from the vent to 5–8 m at the flow front. The morphology is mainly 'a'ā. The 1988–1990 lava flow has a volume of 2.3×10^8 m^3, a maximum length of 10.2 km and was emplaced in 330 days, with peak effusion rates of ~80 m^3/s. The flow has a mean width of 600 m and thicknesses that increase from 10 to 15 m near the vent to >50 m at the front. The morphology varies from 'a'ā in proximal sectors to blocky in the rest of the flow. We modelled the advance rate and thickness of these flows assuming two possible dynamical regimes: An internal rheology regime modelled as a Herschel-Bulkley (HB) fluid and a Yield Strength in the Crust (YSC) regime. We compared our results with the widely used Newtonian and Bingham rheologies. Our results indicate that the 1971 flow can be modelled either by the HB, Bingham or Newtonian rheologies using a single temperature, while the 1988–1990 flow was controlled by the YSC regime. Our analysis and comparison of models shows that care should be taken when modelling a lava flow, as different rheologies and assumptions can reach the same results in terms of advance rate and flow thickness. These examples suggest that the crustal strength should be taken into account in any model of lava flow advance.

1. Introduction

Lava flow morphology depends on different factors acting on the evolution of the flow such as topography, rheology, cooling effects and effusion rate. Different lava morphologies such as pahoe-hoe, 'a'ā and Blocky, result from the interplay between these factors. In consequence, any model that tries to simulate the advance rate or thickness of a lava flow should take into consideration the type of flow that is being modelled, as the dominant dynamics could be different for each case. During the last decades, numerous models have been applied to simulate the advance of lava flows (e.g. Ishihara et al., 1992; Del Negro et al., 2008; Vicari et al., 2009; Fujita and Nagai, 2015). Typically, these models use relationships that calculate the temperature and rheology of the lava in order to calculate the advance rate using a Newtonian or Bingham rheology. These models consider the external crust only for the dynamics of cooling but do not include the effects of the crust on the balance of forces that drives the flow advance, although many authors pointed out the importance it could have (Iverson, 1992; Griffiths and Fink, 1993; Kerr and Lyman, 2007; Takagi and Huppert, 2010, Castruccio et al., 2013). Another issue is that the flow advance is concentrated at the flow front, a zone with a complex thermal structure, where the cooling rate could be different from the channel that is feeding it. Finally, numerous studies have shown that crystal-bearing lavas possess a rheology that has both a pseudoplastic behaviour and/or yield strength (i.e. Pinkerton and Sparks, 1978; Pinkerton and Norton, 1995; Ishibashi, 2009; Vona et al., 2011). Consequently, any model of lava flow advance should take into account these considerations.

In this work we analyze the field characteristics of two lava flows from volcanoes of the Southern Andes of Chile: the 1971 lava flow from Villarrica volcano and the 1988–1990 Lonquimay flow. These flows were emplaced under very different conditions. The Villarrica flow was the result of a Hawaiian eruption with a very high peak effusion rate (>500 m^3/s) and was emplaced in two days, reaching 16.5 km from the vent. The Lonquimay lava flow was generated by a long lasted eruption (~1 year), with a lower peak effusion rate (<100 m^3/s), reaching a distance of 10 km from the vent. In order to investigate

* Corresponding author at: Departamento de Geología, Universidad de Chile, Plaza Ercilla 803, Casilla 13518, Santiago, Chile.
E-mail address: acastruc@ing.uchile.cl (A. Castruccio).

http://dx.doi.org/10.1016/j.jvolgeores.2016.09.015
0377-0273/

if these differing conditions implied a different dynamical control, we simulated the advance rate and thickness of the flow with two models: A 2-D model for Herschel-Bulkley fluids presented in Castruccio et al. (2014) and a crustal yield strength regime (Castruccio et al., 2013). We also compared the results with the widely used Newtonian and Bingham rheologies in order to analyze the possible advantages of each model. Our results indicate that the dynamical control was different in each case.

2. The lava flows from the 1971 and 1988–1990 eruptions from Villarrica and Lonquimay volcanoes

Villarrica and Lonquimay volcanoes are located in the Southern Andes of Chile and are 2 of the most active volcanoes of this area (Fig. 1a). Villarrica volcano (39°S) is composed mainly by products of basaltic-andesite composition. The last eruptions were in 2015, 1984, 1971, 1964, 1963 and 1948. The styles of these eruptions were mainly Hawaiian–Strombolian, with the occurrence of lava flows, lahars and limited ashfall (Moreno and Clavero, 2006). Lonquimay volcano (38°S) is composed essentially by andesitic products. Its last eruptions were in 1988–1990, 1887–1889, 1853 and ~1750. These events were characterized by the emission of voluminous (~0.1 km^3) lava flows and moderated ashfall. These eruptions were not emitted by the main stratocone, but from lateral vents in the NE flank of the volcano.

2.1. The 1971 eruption

The eruption began on 29 October 1971 with very weak activity, consisting on small Strombolian explosions and the effusion of small lava flows that reached the base of the edifice (González, 1995; Moreno and Clavero, 2006). This activity continued intermittently for 2 months. The eruptive cycle culminated during the night of December 29, when a 2 km long eruptive fissure opened across the volcano, generating 2 lava fountains in the NE and SW flanks with an estimated height of 600 m (Fig. 1b). This activity melted the ice and snow covering the volcano, generating lahars in almost all the drainage of the volcano, causing the loss of at least 20 lives and destruction of infrastructure (Moreno and Clavero, 2006). The intensity of the activity decreased considerably after the initial 6–8 h (Moreno, pers. commun.) and the eruption finished 48 h after the beginning of the lava fountaining. The eruption generated 2 lava flows (Fig. 1c): a 6 km long lava flow in the Pedregoso valley (NE flank) and a 16 km long lava flow in the Chaillupen valley (SW flank) with a total estimated volume of ~50 × 10^6 m^3 of basaltic-andesite (52% SiO_2) lavas.

2.1.1. Chaillupen valley lava flow

The lava that flowed down through the Chaillupen valley reached a distance of 16.5 km from the main crater of the volcano and it is classified as a simple lava flow according to the nomenclature of Walker (1972). The flow was strongly confined by the valley topography, with widths rarely exceeding 150 m (Fig. 2). Lava thicknesses vary between 4 and 12 m, depending mainly on the confinement of the flow. The lava was emplaced on slopes that vary between 2° and 5°. The morphology of the flow is mainly ʻaʻā, but in many places there are characteristics that resemble the slabby and rubbly pahoe-hoe textures described by Guilbaud et al. (2005). The emitted lavas have a 52% of SiO_2 (Moreno and Clavero, 2006) and macroscopically they have a hypocrystalline and porfiric texure with 20–30% of plagioclase and olivine phenocrysts and about 5–20% of vesicles. According to the distance to the vent, geometry and morphology of the flow, we divided the lava in 3 sectors: proximal, intermediate and distal.

2.1.1.1. Proximal sector. This section extends from 5 km from the vent (there are no exposed lava in sections closer to the vent) to 9 km. The mean slope of the terrain is 6.7°. The mean thickness of the lava is 12 m and the mean width is 180 m. In this sector, the exposed lava corresponds mainly to levees that are developed on the lateral edges of the valley, as the central channel was almost totally drained and it is covered in many places by late lahar deposits (Fig. 3a). The levees have external walls up to 4 m high, with slopes of 30°. These walls are composed by a matrix-free, moderately to well sorted breccia. The blocks are red to reddish brown and have a mean diameter of 30 cm

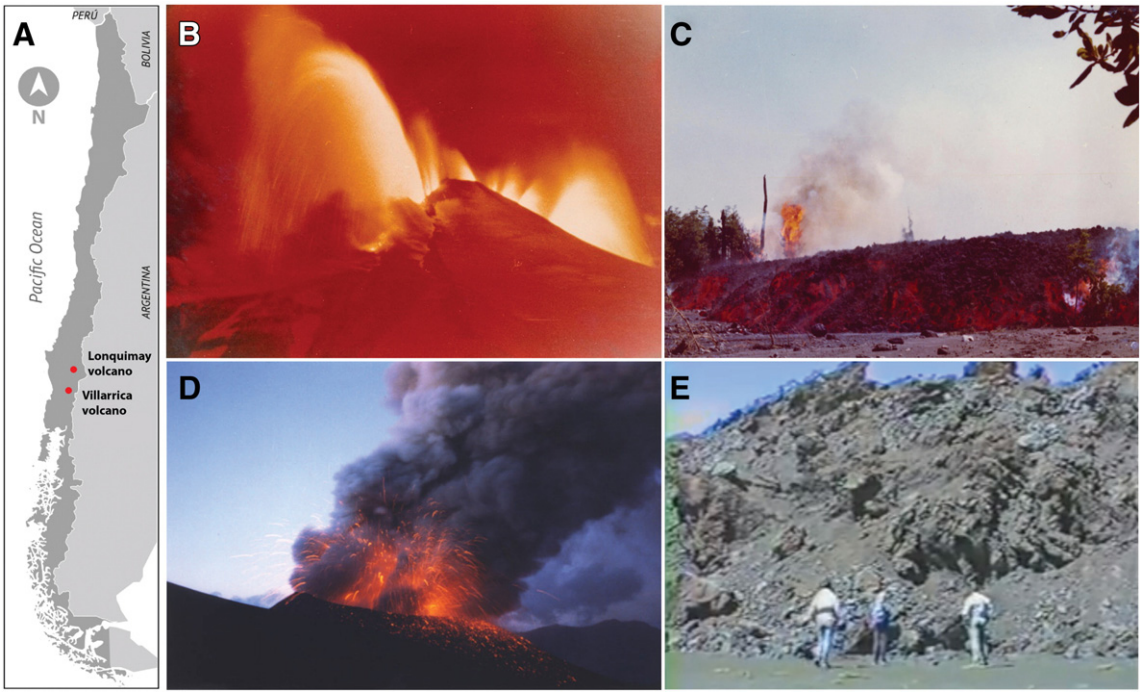

Fig. 1. A) Map of Chile and location of Lonquimay and Villarrica volcanoes. B) ~ 500 m high lava fountain at Villarrica volcano during the night of 29–30 December 1971C) Front of the 1971 flow in the Chaillupén valley. Flow is 5–7 m high. D) 1988–1990 eruption at Lonquimay volcano. The eruption formed a new pyroclastic cone located 3.5 to the NE of the volcano summit. E) Front of the 1988–1990 lava flow in the Lolco valley. Flow is 10–15 m high. (Figs. B) and C) with permission of the Ilustre Municipalidad de Villarrica. D) and E) with permission of www.enlonquimay.com).

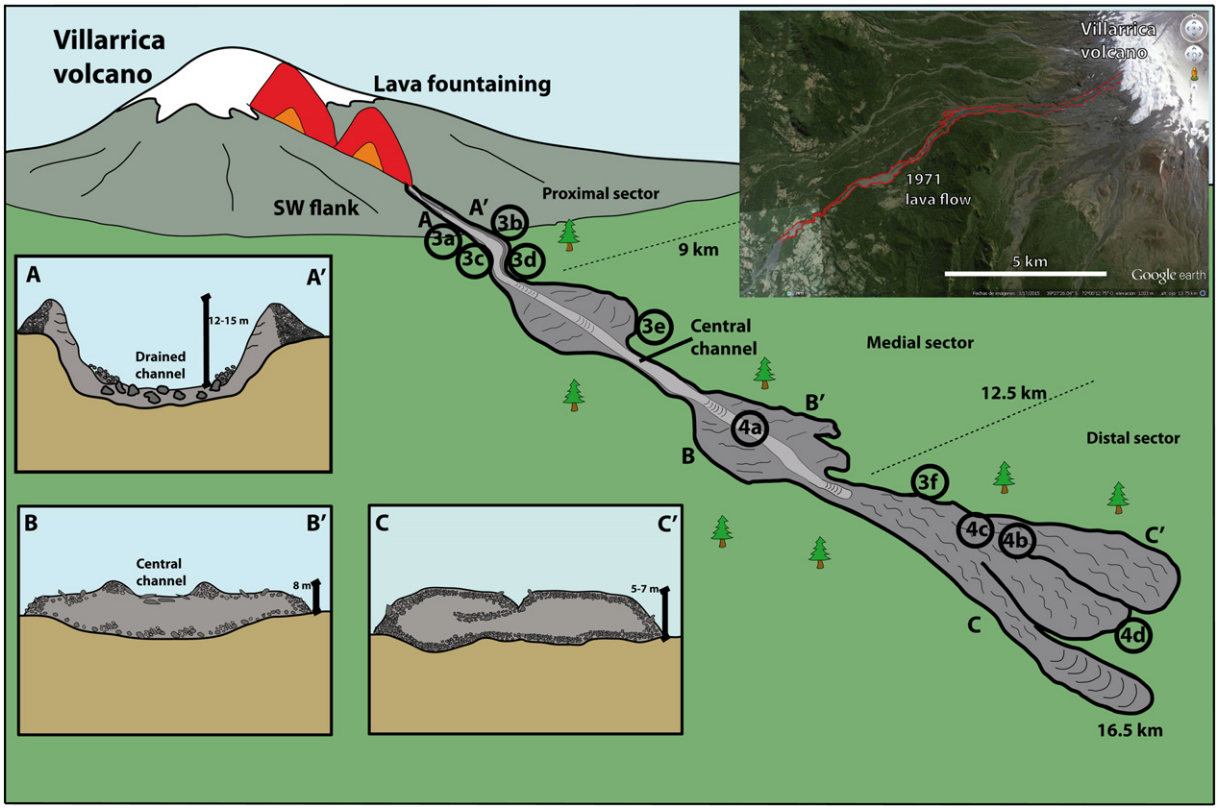

Fig. 2. Cartoon showing the main morphological features of the 1971 lava flow at Villarrica volcano in the Chaillupén valley. Numbers indicate the location of photographs from Figs. 3 and 4.

with bigger blocks up to 1 m (Fig. 3b). These blocks are angular to subrounded with irregular faces. The internal walls of the levee are typically much steeper, with slopes >60° and thicknesses up to 15 m from the central channel floor. These walls are usually composed by different levels of massive lava and welded fragments forming a very irregular surface (Fig. 3d). In some places the inner walls are covered by a 10—12 cm thick vertical crust of massive lava which is coating the levee inner walls which are convoluted and ropy (Fig. 3d). After 7 km from the crater the levees appear only above the valley walls, showing the typical breccia-massive-breccia texture of 'a'ā flows in the inner walls. There are some small overflow lobes <200 m long, 50 m width and 3–4 m thick (Fig. 3c). The blocks and fragments that compose these lobules are welded, showing vertically arranged slabs and extrusions of small spines (<1 m), with little loose rubble.

2.1.1.2. Intermediate sector. This section extends from 9 km from the vent to 12.5 km. The mean slope of the terrain is 4.3°. The mean thickness of the lava is 6–8 m (Fig. 3e) and the mean width is 270 m. In this sector, the lava is less confined by the channel, reaching widths up to 330 m. The central channel has widths of 70–80 m and the top of this channel is only a couple of meters lower than the levees. The central channel is characterized by a tenuous development of transversal ridges, with a wavelength of <5 m and amplitude of <1 m. In some sections of the channel zone, the surface texture of the lava is very similar to the slabby pahoe-hoe surface defined by Guilbaud et al. (2005), with slabs of 15–30 cm thick and between 1 and 2 m of length and width with ropy textures on the upper part (Fig. 4a) and groove marks in the lower face (Fig. 4b). These slabs are usually rotated and emplaced in an imbricated position (Fig. 3f). The levees are much wider than in the proximal sections with widths up to 150 m. The levee surface is characterized by the presence of open fractures up to 1 m wide, usually with a direction perpendicular to the direction of the flow (Fig. 4c). In most of the levees, the surface texture is characterized by irregular, moderately welded clinker ranging in size from 5 cm to 2–3 m (Fig. 3e). This clinker is usually more vesicular in the outer zone (outer 10 cm), with up to 10–20% of vesicles up to 2–3 cm which can be spherical or elongated.

2.1.1.3. Distal sector. The distal sector extends from 12.5 km to 16.5 km from the vent. The mean slope of the terrain is 4°. The mean thickness of the lava is 5 m and the mean width is 250 m. This zone is characterized by the continuous disappearance of the levees, with a disperse flow morphology according to the definition of Lipman and Banks (1987). The front of the flow is divided in 3 lobules, with the western lobule reaching 800 m further downstream (Fig. 2). The internal vertical structure of the front consists in a single flow unit with the typical breccia–massive–breccia structure of 'a'ā lava flows (Fig. 4d). The levees in this zone are very limited in dimensions and confined to the first kilometer of this sector, with widths of <10 m. The surface of the outer wall of these levees is composed by spherical and rounded rubble up to 30 cm in diameter. In the central part of the flow the fragments are larger (up to 2 m) and correspond to clinker with more irregular forms. In this zone the presence of slabs in the upper part is also common and they usually are rotated and lifted up.

2.1.2. Petrography

We collected 15 samples from 8 points along the flow. The samples were taken at the levees, as they represent lava from the front at the moment the lava first passed through the sample location. Samples were taken from vesicular and non-vesicular parts of breccia fragments as well from massive sections of the lava flow when possible, to see if there are variations in crystal content. Hand samples are dark grey, with a porphyritic texture, with 15–20% of phenocrysts, mainly plagioclase and olivine (Fig. 5a). Vesicularity varies between 5 and 20%. Vesicles are usually spherical with sizes up to 1–2 cm.

Optical microscopy and SEM images show phenocrysts (>1 mm) and microphenocrysts (<1 mm and >0.1 mm) of clinopyroxene and

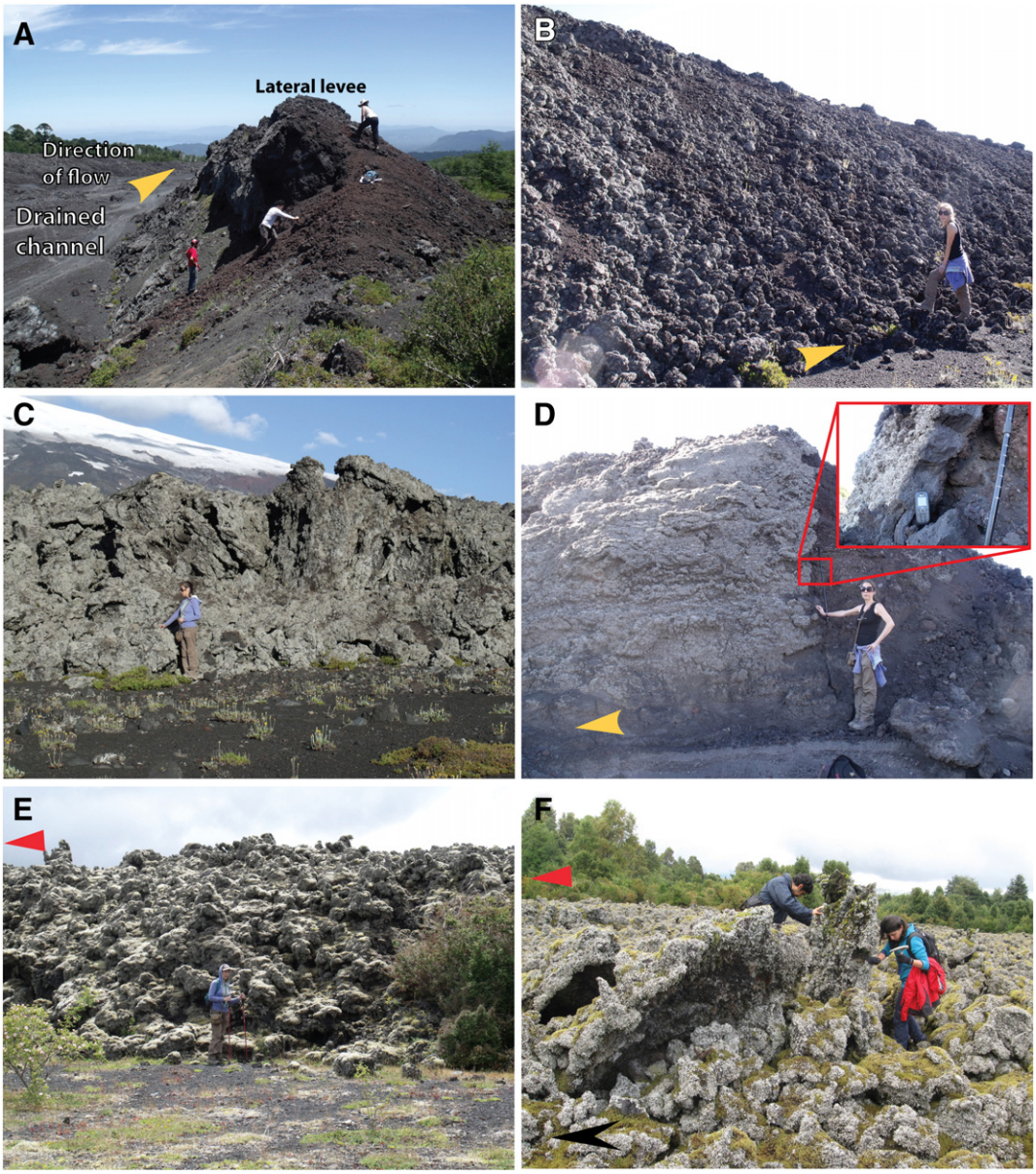

Fig. 3. Photos from the 1971 lava flow in the Chaillupén valley. A) 5 km from vent. Drained central channel and 10 m high lateral levees. B) 5.3 km from vent. Outer wall of lateral levee, composed mostly by rounded rubble. C) 5.5 km from vent. Flow front of a small overflow from the main flow unit. Rubble and slabs are welded. D) 5.5 km from vent. Central channel. Notice the 10–12 cm thick layer of crust that is covering the loose rubble beneath it in the inner wall of the levee. E) 9 km from vent. Outer wall of levee. Rubble is semi-welded and composed by blocks of up to 2 m. F) 12 km from vent. Central channel. Notice the imbricated slabs up to 3 m long.

Fe-Ti oxides in addition to plagioclase and olivine crystals (Fig. 5b and c). Plagioclase crystals are usually euhedral to subhedrals, with sizes <5 mm and aspect ratios (length/width) between 2 and 4. Olivines are <2 mm, euhedrals and with aspect ratios between 1 and 2. The groundmass shows the same mineralogy than the phenocrysts, with very minor amounts of glass. Plagioclase microlites are acicular with aspect ratios between 4 and 10, while clinopyroxenes and Fe-Ti oxides are equant.

Crystal content (phenocrysts + microphenocrysts) varies between 20 and 30%, without showing a clear tendency with distance from the vent (Fig. 5d).

2.2. The 1988–90 Lonquimay eruption

The eruption was preceded by approximately a week of intense seismicity (Moreno and Gardeweg, 1989). The first activity started on 25 December 1988, in a new vent located at 3.5 km to NE of the main summit of the volcano (Fig. 2c). This vent consisted in a 400 m long fissure and the eruption generated an initial column of 5 km of height. During the next days the eruptive column reached 9 km above the surface. The eruptive activity during these first days was mainly vulcanian and was concentrated in the western part of the fissure. A pyroclastic cone started to form reaching a height of 100 m in couple of weeks (Moreno and Gardeweg, 1989). On 27 December, a lava flow started to flow into the Lolco valley, located to the N of the volcano. During the first weeks of January 1989, the intensity of the eruption started to wane and the eruption style shifted to a more Strombolian type and with a continuous supply of lava. During April the cone reached its maximum height of 200 m above the base. The eruption continued during all the year with a progressive decrease in the intensity, with eruptive columns <1 km. Finally in January of 1990 the activity ceased completely (González, 1995).

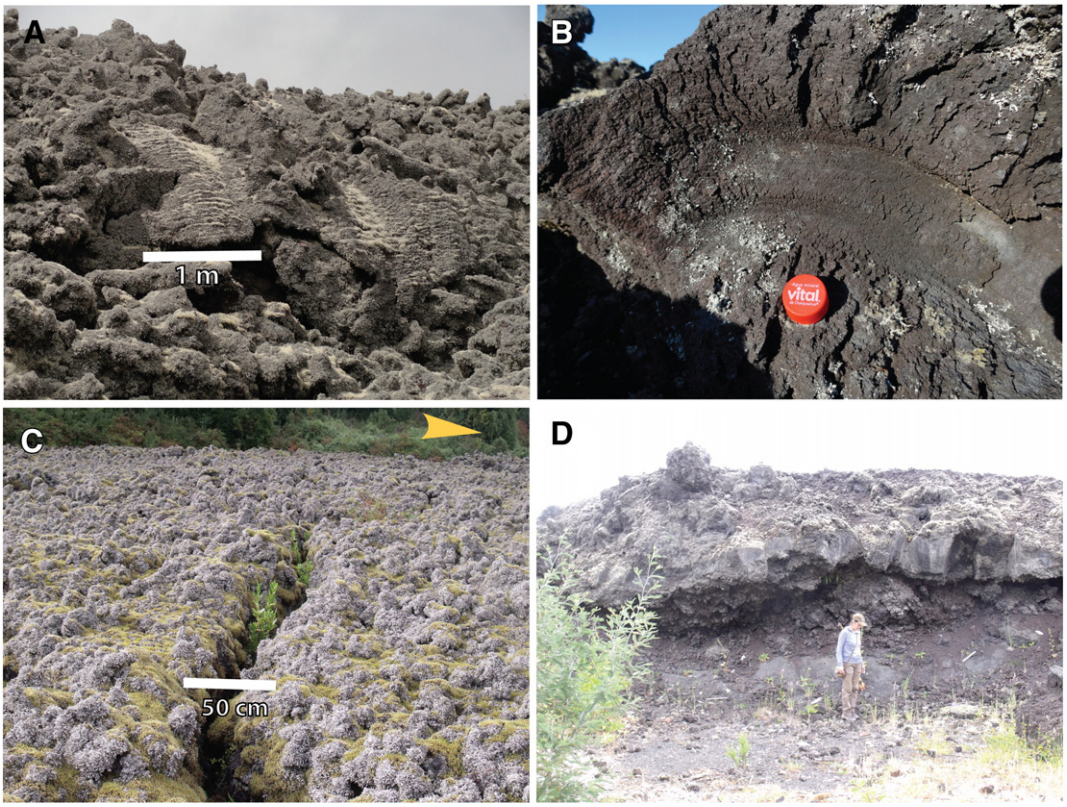

Fig. 4. A) 10 km from vent. Central channel. Upper part of slabs with ropy texture. B) Lower face of an slab with groove marks. C) 14 km form vent. 50 cm wide open fracture perpendicular to the direction of flow. D) 16 km from vent. Flow front with single flow unit with typical breccia- massive-breccia structure of 'a'ā flows.

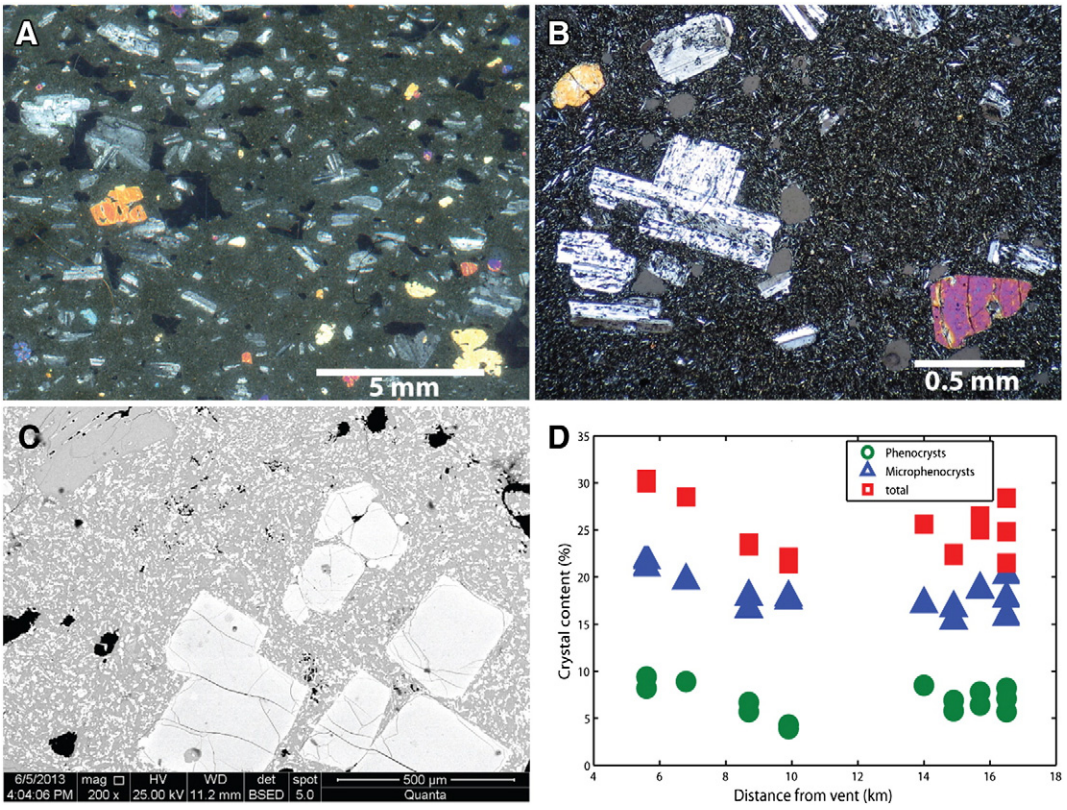

Fig. 5. A) Scan with crossed polar of a thin-section of a sample from the 1971 lava flow. Phenocrysts of plagioclase and olivine. Notice the slight alignment of plagioclase crystals. B) Optical microscope photograph with crossed polar. Phenocrysts of plagioclase and olivine. Notice the abundance of microlites in the groundmass. C) SEM image of the same sample shown in A) and B). Microphenocrysts of olivine and plagioclase in a holocrystalline groundmass composed by microlites of plagioclase, olivine, clinopyroxene and Fe-Ti oxides. D) Crystal content v/s distance of samples from the 1971 flow.

2.2.1. Lolco valley lava flow

The lava flow generated during the 1988–1990 eruption reached a maximum distance of 10.2 km to the N of the vent (Fig. 6). It is also classified as a simple lava flow (Walker, 1972), although in very proximal facies (<1 km from the vent) many subunits are superimposed and a small lobe advanced 1.5 km to the W from the main flow at 2 km from the vent. The flow width was controlled by the valley topography and by the edges of previous lava flows emplaced in the valley. It has a medial width of 600 m, but it reached 1.6 km at the front. The valley slope varies between 6.3° and 0.7°. The thickness of the flow increases from 10 m close the vent to >50 m at the front. The general morphology of the flow corresponds to a blocky lava, although in the proximal sectors the general texture resembles more an 'a'ā flow. The lava has an andesitic composition with a 58% of SiO_2 (Moreno and Gardeweg, 1989). Macroscopically, it has an aphyric texture with <5% of phenocrysts of plagioclase, pyroxene and olivine with a microcrystalline groundmass.

Naranjo et al. (1992) made an excellent description of the main morphological features of this lava flow and here we synthesized some of their observations in addition to our findings of this flow.

2.2.1.1. Proximal sector. The proximal sector covers the lava flow from the vent to 4.5 km downstream. The mean slope of the terrain is 3.5° with a mean flow thickness of the flow of 10 m but in very proximal areas (<200 m from the vent), the thickness could be up to 30 m, with many flow units superimposed. The mean width of the flow is 300 m, although in zones where the flow is bended the width could be up to 800 m (Figs. 6, 7a). In this zone the flow morphology is characterized by a narrow central channel 100–200 m wide, surrounded by up to 4 sets of levees formed by a progressive decrease in the extrusion rate (Fig. 7a, Naranjo et al., 1992). The top of the central channel is usually at a much lower (>5 m) level than lateral levees, with a surface texture of a 'a'ā breccia. In the first meters of the flow (500 m from the vent), Naranjo et al. (1992) describe an "armadillo structure" characterized by an updoming of the surface and Reidel shear structures. The presence of transversal ridges on the surface is very common, with an amplitude of 2–3 m and a length of 15–20 m. Levée surfaces are composed by varying amounts of irregular and vesiculated clinker, typical of 'a'ā lavas, and more dense and angular blocks. The internal structures of levees could be very complex as usually is composed by many units with different textures such as 'a'ā (breccia-massive-breccia) or sheared foliated lava (Naranjo et al., 1992).

2.2.1.2. Intermediate sector. The medial sector extends from 4.5 km to 8 km from the vent. The mean slope is 3.3°, with a mean width of 600 m, varying between 1000 and 300 m. The thickness of the flow increases gradually from 12 to 35 m. This sector is characterized by a single flow unit and a straight channel. The left side of the flow is confined by the valley topography while the right side is self-confined by its levees (Fig. 7b). The width is strongly dependent on the slope as in a sector with a slope of 6–7° at 7 km from the vent, the flow reaches its minimum width (300 m). The central channel–levee morphology is fully developed, but levee structures are simpler as the flow is composed only by one flow unit. The central channel surface is composed by a series of ridges with an amplitude of 5–12 m and a length of 30–50 m (Fig. 7d). The texture of both central channel and levees is mainly typical of blocky lavas, with angular blocks with smooth surfaces and up to 2–3 m, although in some places the surface texture of the lava flows is closer to 'a'ā (Fig. 7c), with clinker and smaller blocks. In this sector there are some occasional spines protruding from levees, with heights that can be up to 6 m.

2.2.1.3. Distal sector. The distal section extends from 8 to 10.2 km from the vent. The mean slope of the terrain is 1.8°. The flow widens progressively from 680 to 1790 m, being confined mainly by the valley topography. The thickness of the flow increases from 35 to 55 m towards the front. In this zone, the central channel–levee division gradually disappears towards the front and the morphology is similar

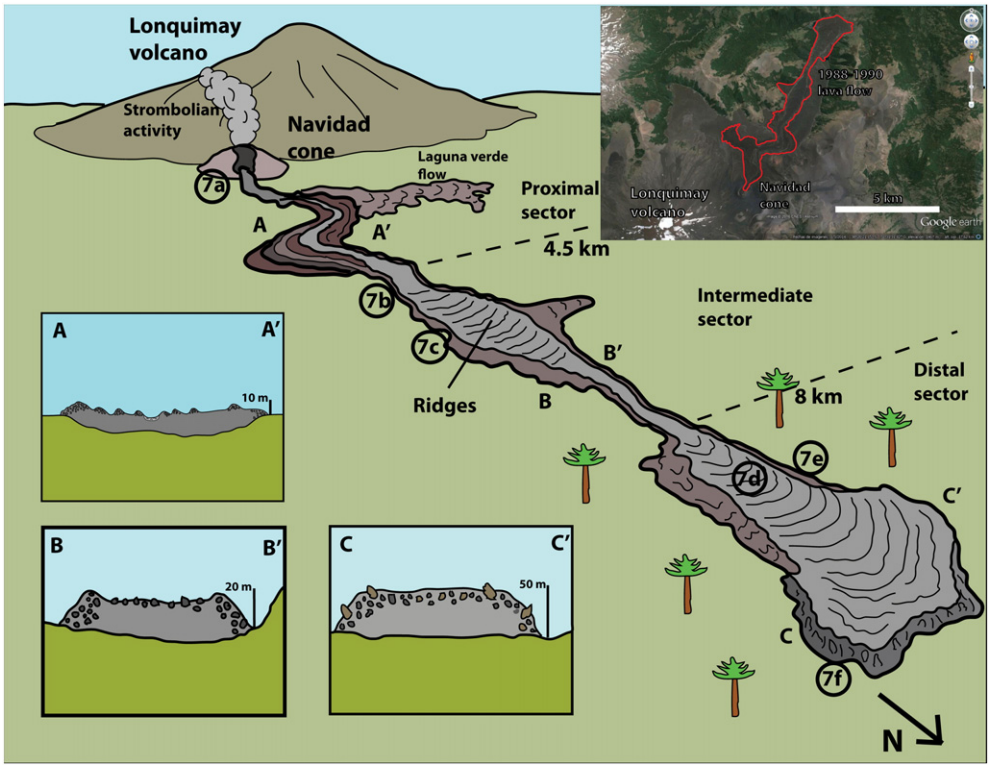

Fig. 6. Cartoon showing the main morphological features of the 1988–90 lava flow at Lonquimay volcano in the Lolco valley. Numbers in circles indicate the location of photographs shown in Fig. 7.

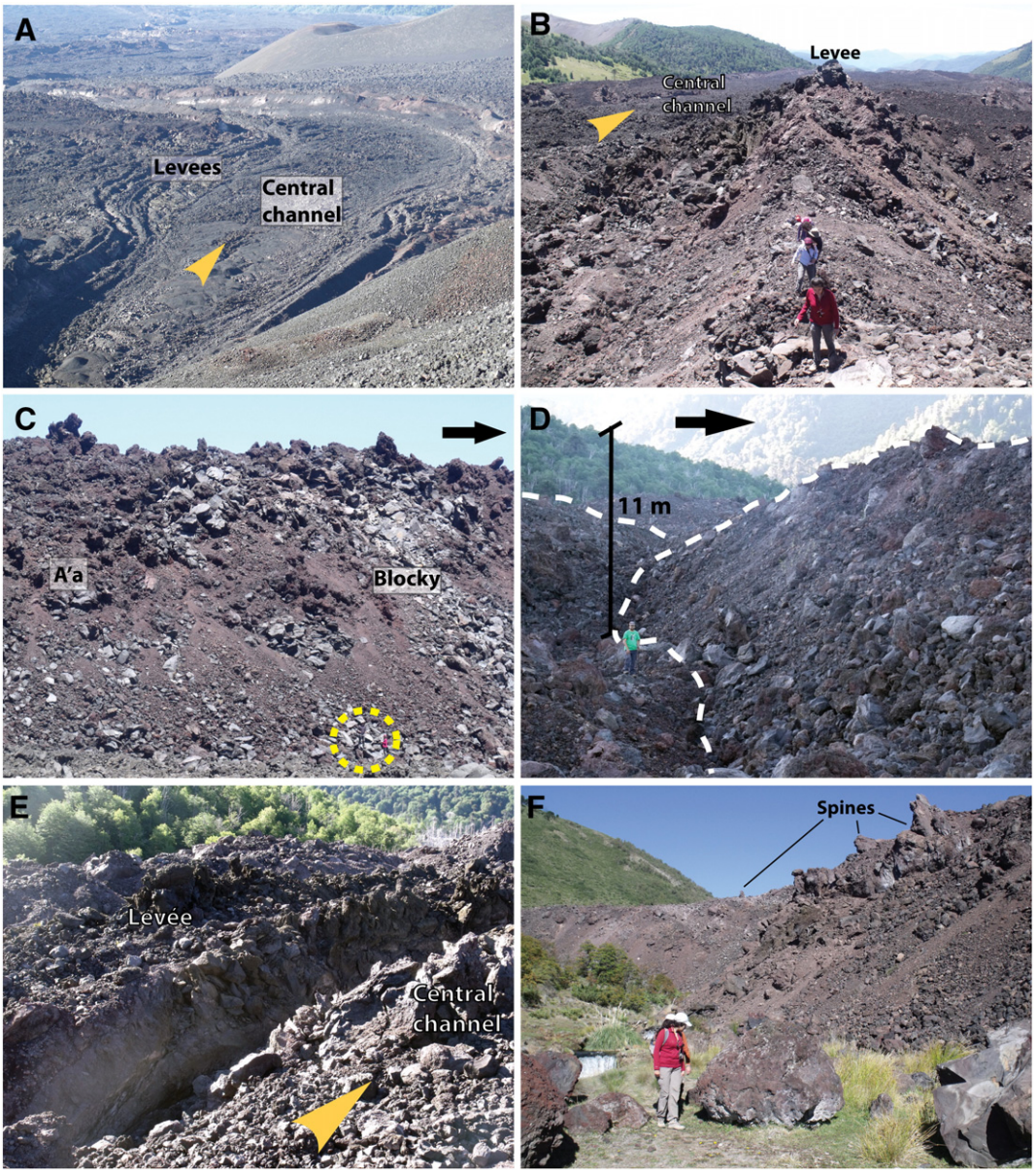

Fig. 7. A) View from the crater of the 1988–1990 pyroclastic cone. Notice the set of levees to the left of the central channel. B) View from top of lateral levee with central channel to the left in the intermediate sector. Levee is 15 m high. C) 18 m outer levee wall from the intermediate sector. Darker clasts have an 'a'ā texture, while lighter blocks are denser, more typical of a blocky morphology. Notice persons for scale in circle D) 11 m high ridge in central channel at 8.5 km from the vent. E) Sharp contact between central channel and lateral levee at 8.5 km from vent. Inner walls of lateral levees are mostly massive. F) Flow front at 10.2 km from vent. The flow is 55 m high. Notice the presence of spines 5–10 m high towards the top of the flow.

to the "disperse flow" region of Lipman and Banks (1987). The contact between the levees and central channel is very sharp, separated by deep fractures (Fig. 7e). The internal walls of the levees are vertical and massive, opposed to the blocky texture of the rest of the flow. The surface texture of the lava is mainly blocky, with fragments up to 5–6 m (Fig. 7d–f). In the surface, ridges are up to 12–14 m in amplitude with lengths of 30–40 m. Spines are abundant in the levees and at the front, with heights up to 10 m (Fig. 7f).

2.2.2. Petrography

We collected 16 samples from 10 points along the flow. Samples were taken from vesicular and massive parts of fragments in order to compare their textures. Hand samples have a dark grey color with an aphanitic texture, with 1–2% of phenocrysts of plagioclase which are <5 mm length (Fig. 8a). Vesicularity varies between 0 and 11%, with individual vesicles <6 mm. Vesicles are mainly spherical but in some places are elongated in the direction of flow.

Optical microscopy and SEM images reveal a porphyritic texture (Fig. 8b and c), with phenocrysts (>1 mm) and micro-phenocrysts (<1 and >0.1 mm) of plagioclase, olivine and clinopyroxene and Fe-Ti oxides. Plagioclase phenocrysts are euhedral, 5 mm maximum length, with a length/width ratio between 4 and 10. Olivines and clinopyroxene are anhedral, with sizes <0.3 mm and a mean aspect ratio of 2.The groundmass has an intergranular texture and it is composed by microlites of plagioclase, clinopyroxene and Fe-Ti oxides and minor amounts of glass. Microlites of plagioclase usually are euhedral and acicular, with aspect ratios between 3 and 10, while the rest of microlites are subhedral and with equant shapes.

The estimated crystal content for each sample is shown in Fig. 8d. The content of phenocrysts and micro-phenocrysts varies between 28

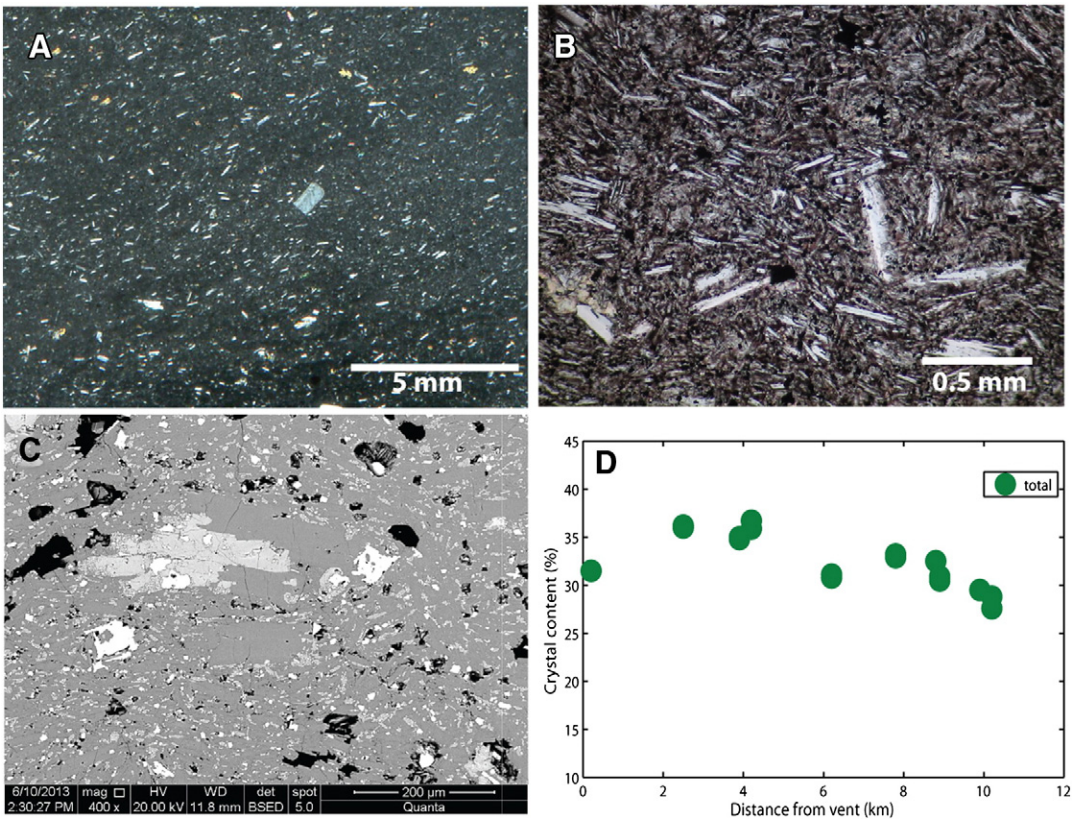

Fig. 8. A) Scan with crossed polar of a thin-section of a sample from the 1988–90 lava flow with microphenocrysts of plagioclase. Notice the alignment of plagioclase crystals. B) Optical microscope photograph with crossed polar. Phenocrysts of plagioclase. Notice the abundance of microlites in the groundmass and the large length/width ratios of plagioclases. C) SEM image of the same sample of A) and B). Microphenocrysts of clinopyroxene and plagioclase in a holocrystalline groundmass composed by microlites of plagioclase, clinopyroxene and Fe-Ti oxides. D) Crystal content v/s distance of samples from the 1988–1990 flow.

and 37%. There is a slight decrease of crystal content with distance from the vent and there are no noticeable differences between samples taken from brecciated and more vesicular parts compared with massive sections of the lava flow.

3. Advance modelling of lava flows

For the two lava flows studied in this work, we noticed that the 1971 Villarrica flow has an 'a'ā morphology, a flow thickness that decreases with distance, an almost empty central channel in proximal facies and extensional structures in the surface. On the other hand, the 1988–1990 Lonquimay flow has a transitional morphology from 'a'ā to blocky, with a thickness that increases towards the front and compressional structures such as notorious ridges and spines in distal facies. In order to understand better the possible mechanisms that originate these morphological characteristics, we simulated the advance rate and dimensions of these two flows with 2 models that consider different controls on the advance of a flow. During the last decades, numerous lava flow models have been used to replicate the advance of flows (e.g. Ishihara et al., 1992; Wadge et al., 1994; Harris and Rowland, 2001; Proietti et al., 2009; Cordonnier et al., 2015; Del Negro et al., 2015; Kelfoun and Vallejo-Vargas, 2015). Most of these models simulate lava flows as Bingham fluids and calculate the rheological parameters (plastic viscosity and yield strength) as a function of composition, temperature and crystal content of the fluid. Despite the usually good matches between the actual and predicted advance rates of the simulated flows, these models do not incorporate the effects of a growing crust on the advance resistance and the estimation of the yield strength of a lava from its crystal content could be highly problematic (e.g. Hoover et al., 2001; Mueller et al., 2009; Castruccio et al., 2010). Here we followed the approaches of Castruccio et al. (2013 and 2014) in order to discriminate if the two lava flows studied here are controlled by the internal rheology or by the external growing crust.

Castruccio et al. (2014) showed that the rheology of many lava flows can be approximated with the Herschel-Bulkley (HB) model:

$$\tau = \tau_y + K\dot{\gamma}^n \tag{1}$$

Where τ is the applied stress and $\dot{\gamma}$ is the strain rate. The rheological parameters are K = consistency, τ_y = yield strength and n, which is a power law exponent. The same authors showed that for a 2-D flow (which is a good approximation when the width of the flow ≫ thickness) the mean velocity is:

$$\overline{u} = \frac{H^2 \rho g \ \sin\ \beta}{3K}\left(\frac{3n}{H^3(n+1)}\left(\frac{\rho g \ \sin\ \beta}{K}\right)^{\frac{1-n}{n}}\right) \times \left(H(H-h_c)^{\frac{n+1}{n}} - \frac{n}{2n+1}(H-h_c)^{\frac{2n+1}{n}}\right) \tag{2}$$

Where H = flow thickness, ρ = lava density, β = terrain slope and $h_c = \frac{\tau_y}{\rho g \sin\beta}$ is the thickness of the plug region (Dragoni et al., 1986). Notice that if $h_c = 0$ and $n = 1$ (Newtonian fluid) we recover the well-known Jeffreys' equation:

$$\bar{u}_{-} = \frac{H^2 \rho g \sin\beta}{3K} \tag{3}$$

If $h_c > 0$ and $n = 1$ we get the 2-D mean velocity of a Bingham fluid (Dragoni et al., 1986):

$$\bar{u}_- = \frac{H^2 \rho g \sin\beta}{3K}\left(1 - \frac{3H_c}{2H} + \frac{H_c^3}{2H^3}\right) \quad (4)$$

On the other hand, Griffiths and Fink (1993), Lyman and Kerr (2006), Takagi and Huppert (2010) and Castruccio et al. (2013) have shown through scaling analysis that under certain conditions, the yield strength of a diffusively growing crust can control the advance of a flow. Castruccio et al. (2013) presented the following relationship:

$$\bar{u}_- = \frac{Q}{W}\left(\frac{\rho g \sin\beta}{\sigma_c \sqrt{\kappa t}}\right)^{\frac{1}{2}} \quad (5)$$

Where, σ_c = yield strength of the crust, κ is the thermal diffusivity of the lava and W is the width of the flow.

Thus, the advance of a lava flow could be controlled by the internal rheology that we are modelling as a Herschel-Bulkley fluid (Eq. (2)) or the flow could be dominated by the yield strength of an external crust that is growing due to conductive cooling (Eq. (5)).

Here we modelled the advance of the 1971 and 1988–90 lava flows using Eqs. (2) and (5), in order to reproduce the advance rate and thickness of the flow. We used the following assumptions:

i) The width of the flow is much greater than the thickness of it (2-D assumption)
ii) The advance of the flow is focused at the front region
iii) The flow front is feed by lava coming from the central channel from behind. The central channel is limited laterally by static levees that were originated during the passing of the flow front.
iv) The effusion rate at the vent is equal to the flow rate of lava from the central channel that is feeding the front. This could be not true as a loss of lava could occur during the passing of lava through the channel due to solidification or deviation on secondary flow units. We approximate effusion rate as Q = mean velocity * height * width.
v) The height of the external levee at certain point is correlated with the height that the flow front had at the time it passed through the point.

We discretized the terrain where the lava flowed in a series of cells, the size of each one depending on the variations of slope and width of the flow, assigning to each one a mean terrain slope and width of the flow (Supplementary Material 1). We applied Eqs. (2) and (5) in each step, calculating the thickness of the flow and the time it took for the flow to cover the distance of the cell. The new effusion rate is then calculated according to the time that has passed since the start of the eruption and the process is repeated in the next step.

We stress that modelling of lava flows requires the knowledge of parameters such as initial crystal content, cooling rates, crystallization gradient, etc. that are difficult to constrain and in many cases are taken from data of other volcanoes and can have high uncertainties. Consequently, our results should be seen mainly as a qualitative analysis made to compare the suitability of different rheological models and dynamical controls on lava flow advance rather than an attempt to precisely determine the rheological parameters of each lava flow.

3.1. 1971 Villarrica flow

There are few observations of the 1971 Villarrica eruption regarding the effusion rate and lava advance. Moreno and Clavero (2006) and Moreno (Personal communication) affirm that the eruption lasted 40–48 h and the lava flow in the Chaillupen valley reached its maximum length in the same time, advancing the first 2/3 of its final length very quickly. Considering that the lava has an approximate volume of 23 × 10^6 m this gives a mean effusion rate of 133–160 m^3/s. The same authors claim that the most intense phase lasted 6–8 h at the beginning of the eruption with an intensity of 500–800 m^3/s. After this time, the effusion rate decayed very quickly. Wadge (1981) noticed that the effusion rate of many basaltic effusive eruptions follows an exponential decay of the form:

$$Q = Q_o \exp(-Bt) \quad (6)$$

Where Q (m^3/s) is the effusion rate, t (s) is time, Q_o is the initial effusion rate and B is a constant depending on the magmatic system properties. Using the data shown previously, we can approximate the evolution of the effusion rate of the 1971 eruption with:

$$Q(m^3/s) = 800 \exp\left(-3.2x10^{-5} t(s)\right) \quad (7)$$

In order to use Eq. (2) we need to estimate parameters K, n and τ_y. For a mixture of a Newtonian liquid phase plus a crystal fraction, Φ, K and n can be calculated as (Castruccio et al., 2010):

$$K(\varphi) = \mu_o\left(1 - \frac{\varphi}{\varphi_m}\right)^{-2.3} \quad (8)$$

$$n(\varphi) = \begin{cases} 1 & \varphi \le \varphi_c \\ 1 + 1.3\left(\frac{\varphi_c - \varphi}{\varphi_m}\right) & \varphi > \varphi_c \end{cases} \quad (9)$$

Where μ_o is the liquid viscosity, Φ_m is the maximum packing fraction. Φ_c is the crystal fraction when non-Newtonian behaviour starts to occur and was empirically determined to be $\Phi_c = 0.44\,\Phi_m$ (Castruccio et al., 2010).

The yield strength is the most problematic parameter to determine and multiple relationships have been proposed to estimate it (e.g. Ryerson et al., 1988; Hoover et al., 2001; Saar et al., 2001; Mueller et al., 2009; Castruccio et al., 2010; Moitra and Gonnermann, 2015). Furthermore, there are differences between results from laboratory experiments and measurements on lava flows in the field. Here we chose the parametrization of Dragoni and Tallarico (1994) as it accounts for the limiting value it can attain when $\Phi \rightarrow \Phi_m$ and reproduces well the measured yield strength of basaltic lavas in the field (Chester et al., 1985):

$$\tau_y = \frac{\tau_o}{2}\left(erf\left[\frac{4(\varphi - \varphi_c)}{\varphi_m - \varphi_c} + 2\right] + 1\right) \quad (10)$$

Where we chose the constants inside the *erf* function in order to make that the yield strength begins to appear when $\Phi = \Phi_c$ and reaches its maximum value when $\Phi = \Phi_m$. τ_o is the maximum yield strength the lava can attain, which we estimated at 7000 Pa for the 1971 flow based in the flow thickness of overflow lobes from the main channel.

The liquid viscosity depends mainly on composition and temperature. We calculated the liquid viscosity following Giordano et al. (2008) using the chemical composition of the groundmass (Supplementary Material 1). In this case, the liquid viscosity can be written as:

$$\log(\mu_o) = \frac{1478.2}{T - 701} \quad (11)$$

Where T is the temperature in (°C) and μ_o is the viscosity in Pa·s. The initial temperature was estimated at 1123–1143 °C by Morgado et al. (2015). We chose a value of $\Phi_m = 0.65$ (Castruccio et al., 2014). Crystal content Φ depends on initial content and temperature. We write $\Phi(T)$ as:

$$\varphi = \varphi_e + \frac{d\varphi}{dT}(T_e - T) \quad (12)$$

Where Φ_e and T_e are the crystal content and temperature at the vent during eruption and $d\Phi/dT$ is the crystal content variation with temperature. Supplementary Material 1 shows a compilation of $d\Phi/dT$ from the literature. We chose $\Phi_e = 0.1$ (Phenocryst content) and $d\Phi/dT = 0.008\Phi/°C$, as this value was obtained with the closest conditions to the 1971 flow (Cashman et al., 1999).

In order to simulate the flow, we fitted the stopping time (2 days) and flow thickness by varying the flow temperature. Temperature controls the HB parameters K, n and τ_y through Eqs. (8), (9), (10), (11) and (12). We use a flow density of $\rho = 2500$ kg/m^3. Fig. 9 shows the simulation with the HB model.

The results indicate that the stopping time (2 days) and thickness of the flow can be replicate with a single temperature of 1087 °C (Fig. 9a and c, Table 1), which implies a crystal content of 0.47. In this case, $K = 1.3 \times 10^5$ Pa·s^n, $n = 0.63$ and $\tau_y = 3600$ Pa. For the case when $d\Phi/dT = 0.003\Phi/°C$ (see Supplementary Material 2 for simulation results), the temperature that best fit the data is 1033 °C with a crystal content of 0.4. The rheological parameters are $K = 2.6 \times 10^5$ Pa.s^n, $n = 0.77$ and $\tau_y = 1054$ Pa.

For comparison, we also simulated the advance rate and flow thickness with a simplified Newtonian and Bingham rheologies (Eqs. (3) and (4), Fig. 9a and c, Table 1). The best fit with a Newtonian rheology is using a single temperature of 1076 °C, which implies a crystal content of 0.55 and a viscosity of 6.7×10^5 Pa·s. The Bingham rheology can fit the data with a lava temperature of 1079 °C, which means a crystal content of 0.53, a plastic viscosity of 3.7×10^5 Pa·s and yield strength of 5770 Pa. Table 1 also shows the parameters with $d\Phi/dT = 0.003\Phi/°C$ (see results in Supplementary Material 2).

Next, we simulated the flow with the YSC model (Fig. 9b and d). We simulated the advance of the lava flow with different values of σ_c. The best fit of the duration of the advance (2 days) is done with a $\sigma_c = 7.7 \times 10^5$ Pa. However the observed trend in flow thickness cannot be matched with any crustal yield strength value, as field measurements indicate a decrease in flow thickness from 15 m at 5 km form vent to 7 m at 16 km, but the modelled thicknesses show an increment with distance from the vent. For example, flow thicknesses for the simulation with $\sigma_c = 7.7 \times 10^5$ Pa are 3–6 m for the first 10 km, while measured thicknesses in this distance range are all over 10 m and only after the first 10 km from the vent the thicknesses are better fitted by the model.

Table 1
Parameters used in the simulations of the 1971 Villarrica flow with the HB, Bingham and Newtonian models.

Villarrica 1971 lava flow simulations (best fits)	K (Pa·s^n)	n	τ_y (Pa)	φ	T (°C)
Herschel-Bulkley					
$d\varphi/dT = 0.008$	1.30E + 05	0.63	3600	0.47	1087
$d\varphi/dT = 0.003$	2.60E + 05	0.77	1054	0.4	1033
Bingham					
$d\varphi/dT = 0.008$	3.70E + 05	1	5770	0.53	1079
$d\varphi/dT = 0.003$	5.36E + 05	1	2166	0.44	1021
Newtonian					
$d\varphi/dT = 0.008$	6.70E + 05	1	0	0.55	1076
$d\varphi/dT = 0.003$	6.54E + 05	1	0	0.45	1018

3.2. Lonquimay 1988–90

The Lonquimay 1988–90 eruption emitted 0.32 km^3 (DRE) of material in 13 months of eruption, of which 0.23 km^3 were lava flows (Naranjo et al., 1992). In this case the best approximation of the effusion rate of lava based in the data of Naranjo et al. (1992) is (see Supplementary Material 1):

$$Q(\mathrm{m}^3/\mathrm{s}) = 90{,}000 * t(s)^{-0.6} \quad (13)$$

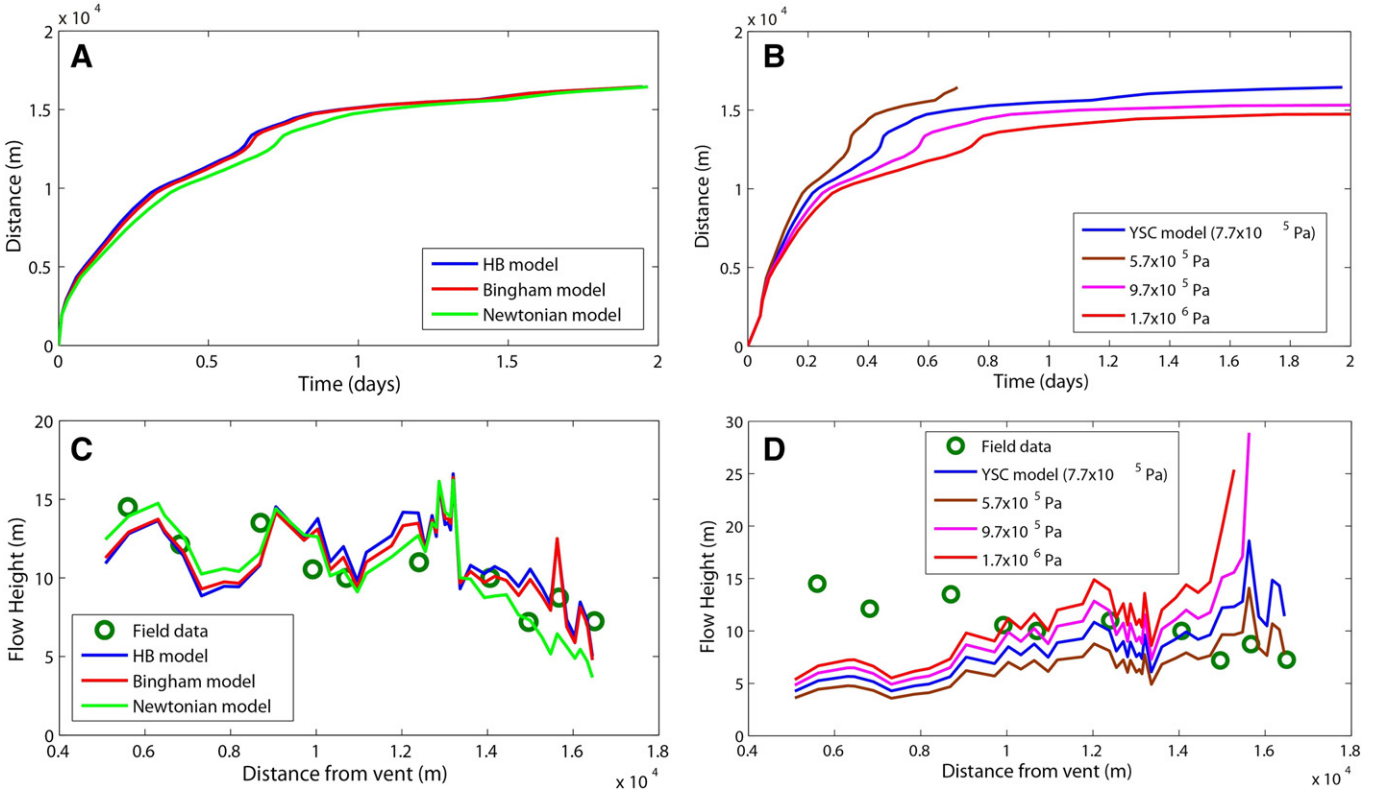

Fig. 9. A) Advance rate simulation of the 1971 flow with the HB, Bingham and Newtonian models. Parameters used are shown in Table 1. B) Advance rate simulation of the 1971 flow with the YSC model using different values for σ_c C) Flow thickness results of simulations shown in Fig. 9A. Thicknesses measured in the field are shown as green circles D) Flow thickness results with the YSC model simulations shown in Fig. 9B.

Table 2
Parameters used in the simulations of the 1988–1990 Lonquimay flow with the HB, Bingham and Newtonian models.

Lonquimay 1988 lava flow simulations (best fits)	Final K (Pa·s^n)	Final n	Final τ_y (Pa)	Final φ	T_e (°C)	T_f (°C)
Herschel-Bulkley						
$d\varphi/dT = 0.008$	3.87E + 06	0.5	12,935	0.41	1080	1067
$d\varphi/dT = 0.003$	8.20E + 06	0.55	11,357	0.39	1054	1019
Bingham						
$d\varphi/dT = 0.008$	6.80E + 08	1	14,935	0.49	1076	1058
$d\varphi/dT = 0.003$	6.19E + 08	1	14,864	0.48	1041	991
Newtonian						
$d\varphi/dT = 0.008$	3.94E + 09	1	0	0.49	1071	1057
$d\varphi/dT = 0.003$	3.33E + 09	1	0	0.48	1037	989

We calculated the liquid viscosity using the glass composition (Supplementary Material 1) and the equations of Giordano et al. (2008):

$$\log(\mu_o) = \frac{2368.6}{T - 576.6} \tag{14}$$

We used $T_e = 1100$ °C (Moreno and Gardeweg, 1989) and μ_o is in Pa·s. We chose a maximum packing fraction of 0.5 as crystals are much more elongated, with aspect ratios up to 10 (Mueller et al., 2009; Ishibashi, 2009). We set $\rho = 2500$ kg/m^3.

In the case of the HB model, we noticed that a reasonable fit of the data can be done with 2 temperatures (Supplementary Material 2): a temperature of 1077 °C for the first 9 days and a second temperature of 1059 °C for the rest of the flow advance time. That the advance rate and thickness of the flow can be modelled with only two temperatures suggest that the flow front temperature reached equilibrium after some time. Next we simulated the flow choosing arbitrarily the following relationship for the front temperature:

$$T = T_f + (T_e - T_f) \times e^{-Ct} \tag{15}$$

Where T_f is the equilibrium temperature and C is a constant. The parameters used for the best fit of the data are shown in Table 2 and the results are shown in Fig. 10a and c. Additional results with $d\Phi/dT = 0.003\Phi$/°C are shown in Supplementary Material 2.

The YSC regime gives an excellent fit of the data for both the advance rate and flow thickness (Fig. 10b and d) with a value of $\sigma_c = 3 \times 10^5$ Pa for the crustal strength. See Supplementary Material 2 for results with changing values of σ_c.

4. Discussions

4.1. Rheological models of lavas

Our simulations indicate that the advance rate and thickness of the 1971 lava flow can be simulated by the HB, Bingham and Newtonian models with a constant temperature. The lava temperature and crystal content are within a range of 11 °C and 0.08 between the three models. It is not possible to select the best fit between the models as the differences observed in thickness and advance rate are within the errors associated to the measurements of these parameters. Similarly, the differences in the temperatures and crystal content obtained from the simulations are also within the uncertainties and errors associated.

The fact that the three rheological models can simulate equally well the 1971 flow would be indicating that the conditions of stress and strain rate of the flow are relatively constant during the fast advance of the flow in the initial stages as according to our simulations 2/3 of the final length of the flow was reached in the first 12 h of the eruption and velocity was almost constant between 5 and 12 km form vent. If the eruption would have lasted longer, then the stress and strain rate conditions would have changed and the results with each model would have

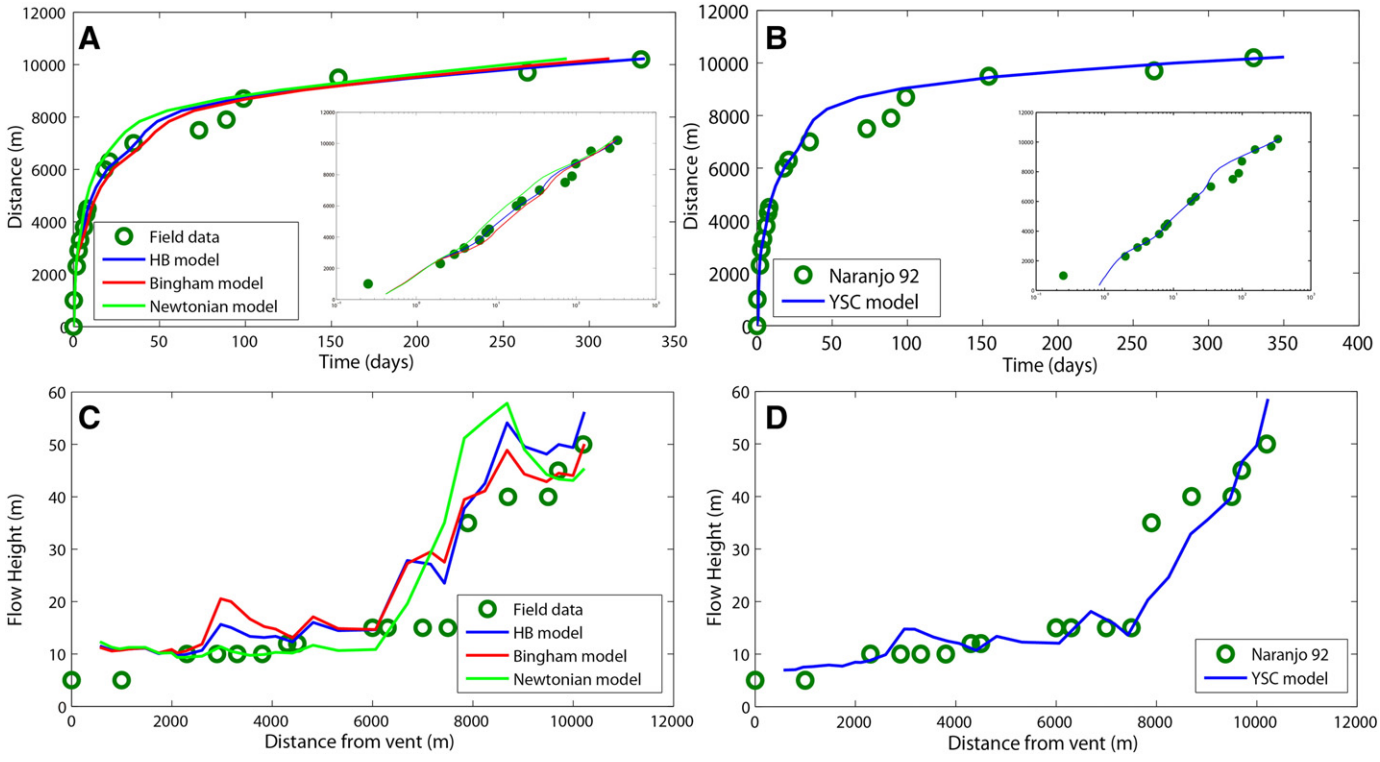

Fig. 10. A) Advance rate simulation of the 1988–1990 flow with the HB, Bingham and Newtonian models B) Advance rate simulation of the 1988–1990 flow with the YSC model C) Flow thickness results of simulations shown in Fig. 10A D) Flow thickness results of simulation shown in Fig. 10B. Insets in Figs. 10A and B show the same data of the same graph but in logarithmic scale.

been different in distal sectors. These results suggest that for fast, short lived lava flows (<2 days) with a short waning phase for the effusion rate, any of the three rheologies are a good approximation for the modelling of the flow.

The YSC proved to be inadequate to model the 1971 lava flow as for none of the simulations was possible to fit the thickness of the flow for the first 10 km, where field measurements show a decrease of thickness with distance, opposed to the simulation results.

In the case of the 1988–1990 Lonquimay lava flow, the three internal rheology models are capable of replicate the advance rate and thickness of the flow. However the crystal content needed in the second half of the flow for both Newtonian and Bingham models is very close to the maximum packing fraction ($\Phi = 0.49$ for $\Phi_m = 0.5$). This high crystal content implies that K will be very sensitive to very small changes in crystallinity as K increases asymptotically to infinity when Φ approaches Φ_m.

On the other hand, the Lonquimay lava flow can also be modelled by the YSC model, with a good fitting for the entire advance rate and thickness of the flow data with a single Yield strength of 3×10^5 Pa. Kerr and Lyman (2007) reached the same conclusions but without considering the terrain slope and with a higher yield strength (2 MPa). Here we showed that the YSC model can also fit the entire thickness of the flow. It is surprising how well the YSC model can predict the sudden increment in thickness from 7500 m of distance from the vent onwards. The yield strength value of 3×10^5 Pa is consistent with previous estimates of the yield strength for siliceous lava flows and domes (Blake, 1992; Fink and Griffiths, 1998; Kerr et al., 2006), which are in the order of 10^5 Pa.

In order to discriminate which of the two models (HB or YSC) is responsible for the advance rate and thickness of a lava flow, we analyzed the forces that act in each case. The yield strength in the crust will dominate over the internal rheology (Herschel-Bulkley) when:

$$\sigma_c \frac{\delta}{H} >> \tau_y + K\left(\frac{\dot{u}}{H}\right)^n \tag{16}$$

Where we approximate the strain rate as $\sim u/H$. Notice that this inequality depends on the rheological parameters, and also on the flow velocity and thickness, that in turn depends on the effusion rate. Fig. 11 shows the minimal effusion rate necessary for the domination of the internal rheology over the YSC regime using different rheological parameters for the Villarrica and Lonquimay cases. In the Villarrica case (Fig. 11a) the HB rheology dominates until ~2 days if $\sigma_c = 5 \times 10^4$ Pa, 1.5 days if $\sigma_c = 10^5$ Pa or 0.7 days if $\sigma_c = 5 \times 10^5$ Pa. In the Lonquimay case (Fig. 11b) the crustal yield strength will dominate after a few days (maximum 6 days) for all the cases simulated. This supports our simulation results. For example, in the 1971 Villarrica simulations with the YSC model, the modelled thicknesses cannot reproduce the field measurements for the first 10 km which means the first 12 h approximately. In the case of the Lonquimay case, the YSC can fit the data after the first 2 days (see the insert of Fig. 10B).

It is also interesting to compare the final Graetz number for both the Villarrica and Lonquimay lava flows. Graetz number (Gz) is a dimensional number that can be written as:

$$\mathrm{Gz} = \frac{d_e^2}{\kappa t} \tag{17}$$

Where d_e is the equivalent diameter (Pinkerton and Wilson, 1994). According to Pinkerton and Wilson (1994) cooling-limited lava flows stop when Gz reached a value between 280 and 370. This means that the flow will stop when the crust thickness is only 5–6% of the equivalent diameter or ~10% of the flow thickness when W ≫ H. This reinforces the idea that the external crust controls the global rheology of a lava flow (Wilson, 1993). In the case of the 1971 Villarrica flow, the lava stopped when Gz = 1058, while the 1988–1990 Lonquimay flow stopped when Gz = 269. These calculations suggest that the Lonquimay lava flow is cooling-limited while the Villarrica flow is volume-limited (Pinkerton and Wilson, 1994; Harris and Rowland, 2009). Thus, according to our results, the modelling of advance rate of cooling-limited lava flows should consider the effects of the growing crust in the balance of forces. Recently, Cordonnier et al. (2015) reviewed different numerical codes to simulate the advance of lava flows and none of them includes the effects of the crust on the dynamical analysis. The results presented here have shown that the lava flow advance rate can be modelled equally well by different rheological models with the appropriate selection of parameters. Thus it is extremely important to analyze the flow conditions of lava before modelling it, as the selection of a lava model based only in the fitting of the advance rate can lead to false conclusions.

4.2. Applicability to ancient flows

The estimation of the eruption rate of ancient flows from lava morphology has been investigated since the pioneering work of Hulme (1974). After him, numerous works have studied the composition and eruption rate of ancient lava flows (e.g. De Silva et al., 1994; Deardoff and Cashman, 2012) or extra-terrestrial lavas (e.g. Hulme and Fielder, 1977; Gregg and Fink, 1996). With the equations presented here, which are a refinement of the work of Castruccio et al. (2014), we can estimate not only the mean eruption rate, but also the variations of this parameter during flow emplacement by measuring lava thickness and width with distance.

For volume limited flows controlled by the internal rheology, the main sources of error are the estimations of the temperature of the flow and crystal content. Flow temperature can be estimated by geothermometers (Cashman et al., 1999; Putirka, 2008) using glass compositions and crystal content can be estimated from counting it on selected samples. However is not simple to estimate how many crystals were originated after emplacement as in the Villarrica samples the groundmass is almost full of microlites, with only traces of glass. We made the exercise of trying to recover the effusion rate for thickness and width data of the 1971 flow using the HB model. Fig. 12a show the results for different estimations of T and Φ. We assume an effusion rate of the form of Eq. (7) and we fitted the thickness data with parameters Q_o and B using a non-linear regression (nlinfit function in MatLab). Results with $\Phi = 0.5$ are closer to the best estimation of the effusion rate (Eq. (11)) and duration of the eruption, with flow durations of 2.5–3.5 days and mean effusion rates of 80–115 m^3/s. On the other hand, results with $\Phi = 0.4$ show shorter flow durations (0.4–0.6 days) and mean effusion rates between 700 and 1100 m^3/s. Thus the estimation of the crystal content during flowing of the lava is critical to better estimations of the effusion rate as it is very sensitive to this parameter.

In the case of the YSC model, it is not possible to estimate the crustal yield strength from lava composition or crystal content, although numerous studies suggest that the value is restricted in the order of ~10^5 Pa (Blake, 1992; Fink and Griffiths, 1998; Kerr et al., 2006). Another possible limitation is the measurement of the terrain slope to estimate velocities and flow rates, as for ancient flows only the post-eruption slope can be measured. For short-lived, high effusion rate basaltic eruptions such as the 1971 Villarrica flow, the error will be low as usually the thicknesses of the flow are thin (~10 m) and the slope at macro-scales (100 s of meters) does not change appreciably. However, for thicker lava flows such as the Lonquimay 1988–1990 flow, the changes in the slope can be noticeable. We tested the error in the recovered effusion rate from the 1988–1990 using only the post-emplacement lava thickness data measured in the field (Fig. 12, see Supplementary Material 2 for advance rate estimation and comparison with data from Naranjo et al., 1992) and terrain slope calculations from the Google Earth elevation model. We assumed an effusion rate of the form $Q = Q_o t^{\alpha}$. We fit thickness data with different values of σ_c (Fig. 12b). The best result is with a crustal yield strength of 3×10^5 Pa.

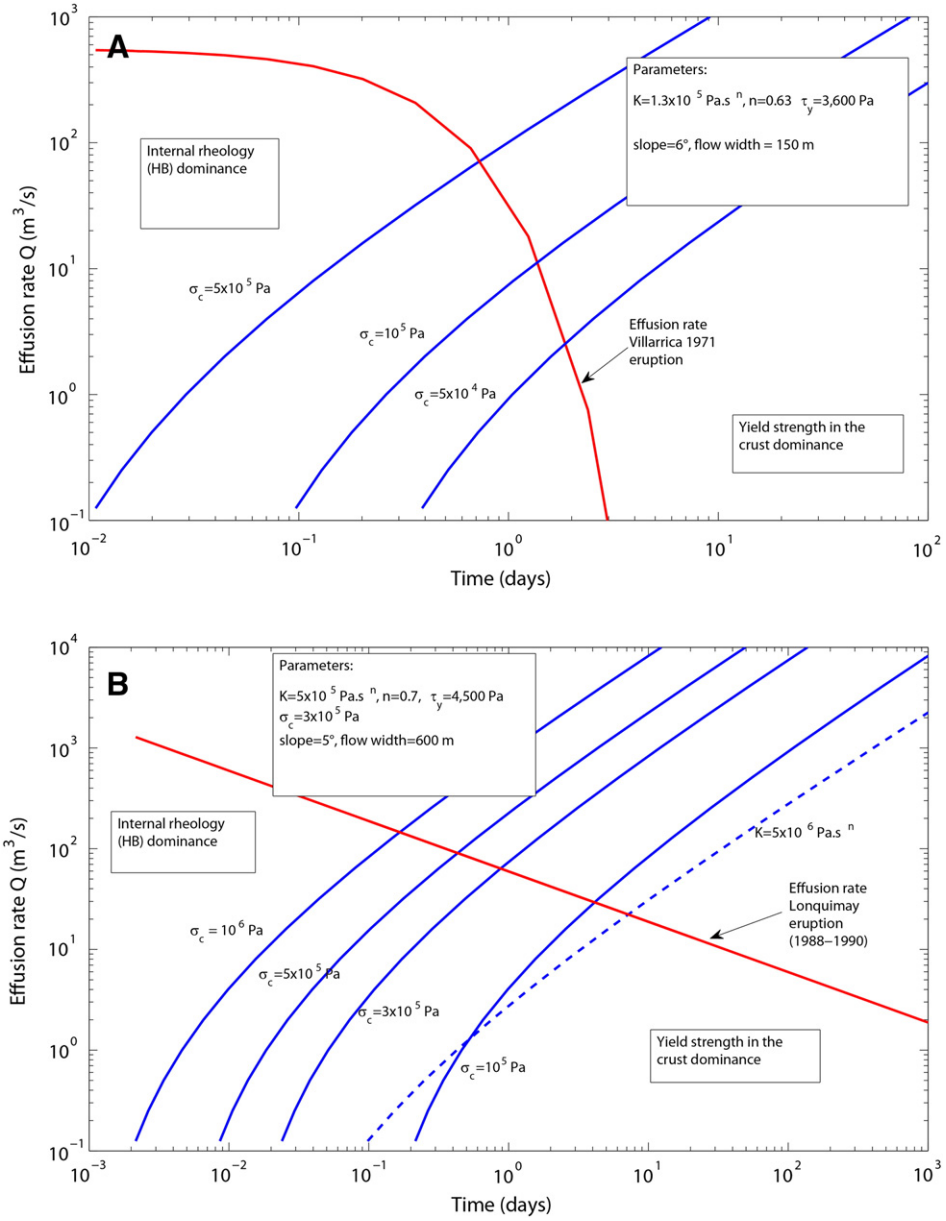

Fig. 11. Minimum effusion rate necessary (blue lines) for the internal HB regime to dominate over the YSC regime for different selection of rheological parameters. Fig. 11A shows the Villarrica 1971 effusion rate (red line) and Fig. 11B shows the Lonquimay 1988–1990 effusion rate.

The calculated duration of the eruption is ~700 days with a mean effusion rate of 6m^3/s. However this is due to an extreme slowing down of the modelled flow in the last 500 m, as according to the fit the flow reached 9.7 km in 300 days, which compares much better with the 264 days of the actual flow. If we considered only the first 95% of the flow, the calculated mean effusion rate is 9m^3/s which compares well with the 10.5 m^3/s calculated from data of Naranjo et al. (1992).

5. Conclusions

Our results indicate that short-lived lava flows (<2 days) can be modelled with a single temperature for the entire flow. Although numerous studies have shown that lavas have yield strength and pseudo-plastic behaviour, the HB rheology does not represent a real advantage in terms of modelling as the differences between the HB, Bingham and Newtonian models are inside the errors associated to measurements of advance rate, thickness of the flow, crystal content and temperature.

The 1988–1990 Lonquimay lava flow can be modelled by the three previously mentioned models assuming an exponential decay in the frontal temperature of the flow. However the Bingham and Newtonian models need crystals contents to be very close to the maximum packing fraction. On the other hand the YSC model can model the advance rate and thickness of the flow with a single parameter for the entire flow.

Analysis of the internal rheology versus the yield strength in the crust show that the YSC regime would dominate after a few days in the case of the Lonquimay flow. Further estimations of the Graetz number for both lavas suggest that cooling limited flows should consider the effects of the growing crust in the advance modelling.

Field analysis reveals that the Villarrica lava has a decrease of thickness with distance, a predominance of ‘a‘ā texture and few structures. On the other hand, the Lonquimay flow shows a clear increase of thickness with distance, numerous compressional structures such as spines and ridges and a transition from ‘a‘ā to blocky morphology. These differences can be useful to discriminate the character (cooling versus volume limited) of ancient lava flows. This is critical when

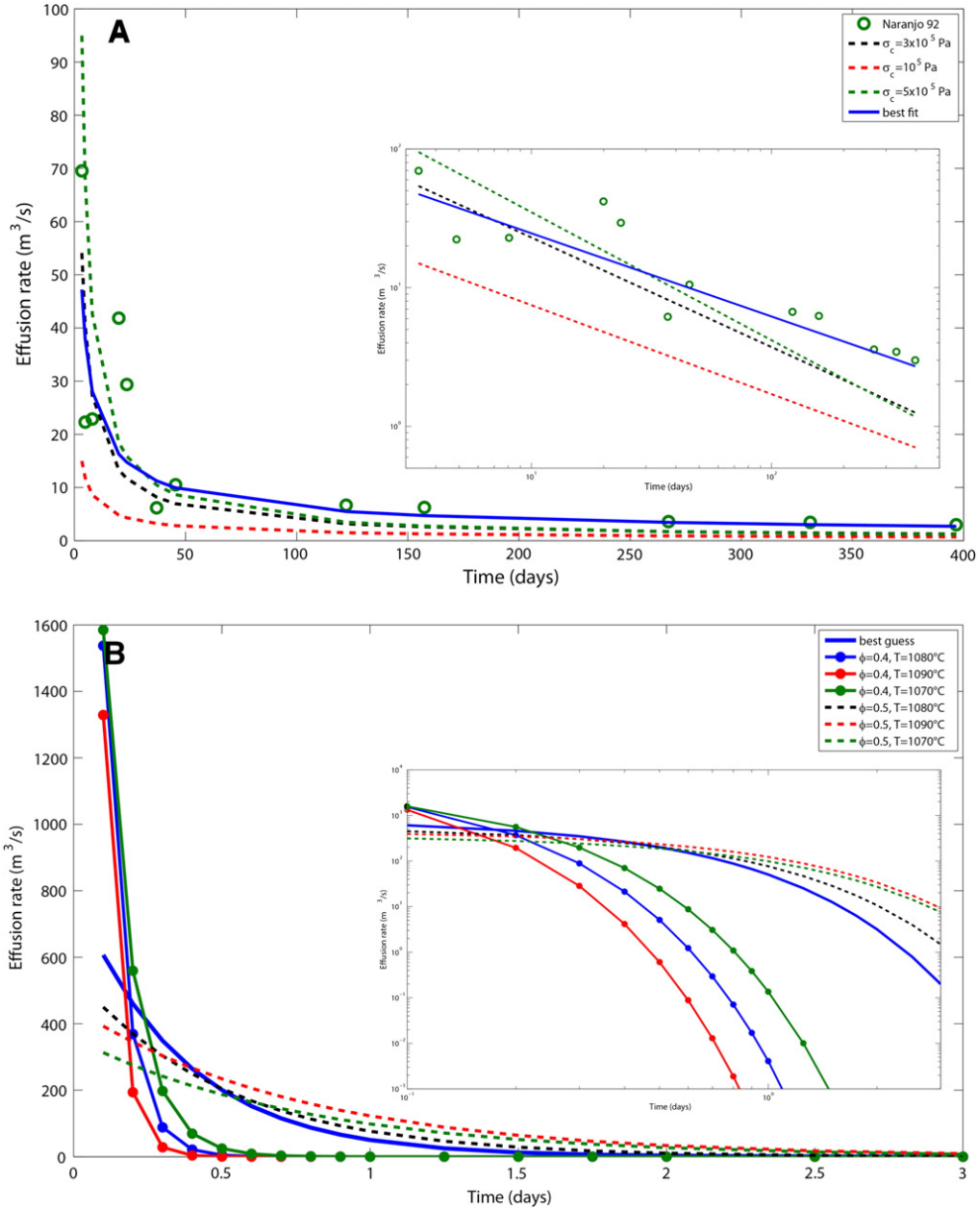

Fig. 12. A) Effusion rates obtained for the 1988–1990 eruption using the YSC model and the thicknesses and width of the flow in the field. The blue line is the best fit of the data of Naranjo et al. (1992). Dashed lines indicate different values for the crustal strength. B) Effusion rates obtained for the 1971 eruption using the HB model and the thicknesses and width of the flow in the field. Blue line indicates the effusion rate based in the accounts of Moreno and Clavero (2006). Dashed and pointed lines indicate the results with different values of flow temperature and crystal content. Insets in both figures show the same data of the main graph but in logarithmic scale.

estimating the effusion rate as these two types of flow are dynamically controlled by different forces acting on distinct parts of the flow.

Estimation of effusion rate from ancient lavas is simpler in the case of cooling limited flows as it requires the estimation of only one rheological parameter, opposed to volume limited flows that requires the estimation of eruption temperature, crystal content and melt composition.

Acknowledgements

AC thanks the FONDECYT project 11121298 and FONDAP project 15090013. We thank CONAF for the access permission to protected areas in both volcanoes. We thank the help on the field of A. Salas, R. Gho, O. Bustamante, G. Pedreros, C. Contreras, E. Morgado, CG. Jorquera and Alejandro Castruccio.

Appendix A. Supplementary data

Supplementary data to this article can be found online at http://dx.doi.org/10.1016/j.jvolgeores.2016.09.015.

References

Blake, S., 1992. Viscoplastic models of lava domes. In: Fink, J.H. (Ed.), Lava Flows and Domes: Emplacement Mechanisms and Hazard Implications. Springer-Verlag, Berlin, pp. 88–128.

Cashman, C., Thornber, C., Kauahikaua, J., 1999. Cooling and crystallization of lava in open channels, and the transition of Pahoehoe Lava to `A`a. Bull. Volcanol. 61, 306–323.

Castruccio, A., Rust, A.C., Sparks, R.S.J., 2010. Rheology and flow of crystal-bearing lavas: insights from analogue gravity currents. Earth Planet. Sci. Lett. 297, 471–480.

Castruccio, A., Rust, A.C., Sparks, R.S.J., 2013. Evolution of crust- and core-dominated lava flows using scaling analysis. Bull. Volcanol. 75, 681. http://dx.doi.org/10.1007/s00445-012-0681-2.

Castruccio, A., Rust, A.C., Sparks, R.S.J., 2014. Assessing lava flow evolution from post-eruption field data using Herschel-Bulkley rheology. J. Volcanol. Geotherm. Res. 275, 71–84.
Chester, D.K., Duncan, A.M., Guest, J.E., Kilburn, C.R.J., 1985. Mount Etna, the Anatomy of a Volcano. Chapman and Hall, London.
Cordonnier, B., Lev, E., Garel, F., 2015. Bechmarking lava-flow models. In: Harris, A.J.L., De Groeve, T., Garel, F., Carn, S.A. (Eds.), Detecting, Modelling and Responding to Effusive Eruptions. Geological Society, London, Special Publications, p. 426. http://dx.doi.org/10.1144/SP426.7.
De Silva, S.L., Self, S., Francis, P.W., Drake, R.E., Ramirez, C., 1994. Effusive silicic volcanism in the Central Andes: the Chao dacite and other young lavas of the Altiplano-Puna volcanic complex. J. Geophys. Res. 99 (B9), 17805–17825.
Deardoff, N., Cashman, K.V., 2012. Emplacement conditions of the c. 1,600-year BP Collier Cone lava flow, Oregon: a LiDAR investigation. Bull. Volcanol. 74, 2051–2066.
Del Negro, C., Fortuna, L., Herault, A., Vicari, A., 2008. Simulations of the 2004 lava flow at Etna volcano using the magflow cellular automata model. Bull. Volcanol. 70, 805–812.
Del Negro, C., Cappello, A., Ganci, G., 2015. Quantifying lava flow hazards in response to effusive eruption. Geol. Soc. Am. Bull. http://dx.doi.org/10.1130/B31364.1.
Dragoni, M., Tallarico, A., 1994. The effect of crystallisation on the rheology and dynamics of lava flows. J. Volcanol. Geotherm. Res. 59, 241–252.
Dragoni, M., Bonafede, M., Boschi, E., 1986. Downslope flow models of a Bingham liquid: implications for lava flows. J. Volcanol. Geotherm. Res. 30, 305–325.
Fink, J.H., Griffiths, R.W., 1998. Morphology, eruption rates and rheology of lava domes: insights from laboratory models. J. Geophys. Res. 103, 527–546.
Fujita, E., Nagai, M., 2015. LavaSIM: its physical basis and applicability. In: Harris, A.J.L., De Groeve, T., Garel, F., Carn, S.A. (Eds.), Detecting, Modelling and Responding to Effusive Eruptions. Geological Society, London, Special Publications 426. http://dx.doi.org/10.1144/SP426.14.
Giordano, D., Russell, J.K., Dingwell, D.B., 2008. Viscosity of magmatic liquids: a model. Earth Planet. Sci. Lett. 271, 123–134.
González, O., 1995. Volcanes de Chile. Instituto Geográfico Militar, Santiago (in spanish).
Gregg, T., Fink, J., 1996. Quantification of extraterrestrial lava flow effusion rate through laboratory simulations. J. Geophys. Res. 101 (E7), 16891–16900.
Griffiths, R.W., Fink, J.H., 1993. Effects of surface cooling on the spreading of lava flows and domes. J. Fluid Mech. 252, 667–702.
Guilbaud, M.-N., Self, S., Thordarson, T., Blake, S., 2005. Morphology, surface structures, and emplacement of lavas produced by Laki, A.D. 1783–1784. In: Manga, M., Ventura, G. (Eds.), Kinematics and Dynamics of Lava Flows: Geological Society of America Special Paper 396, pp. 81–102. http://dx.doi.org/10.1130/2005.2396(07).
Harris, A.J.L., Rowland, S.K., 2001. FLOWGO: a kinematic thermo-rheological model for lava flowing in a channel. Bull. Volcanol. 63, 20–44.
Harris, A.J.L., Rowland, S.K., 2009. Effusion rate controls on lava flow length and the role of heat loss: a review. In: Thordarson, T., Self, S., Larsen, G., Rowland, S.K., Hoskuldsson, A. (Eds.), Studies in Volcanology, the Legacy of George P. L. Walker. Special Publications of IAVCEI No. 2, pp. 33–51.
Hoover, S., Cashman, K.V., Manga, M., 2001. The yield strength of subliquidus basalts: experimental results. J. Volcanol. Geotherm. Res. 107, 1–18.
Hulme, G., 1974. The interpretation of lava flow morphology. Geophys. J. R. Astron. Soc. 39, 361–383.
Hulme, G., Fielder, G., 1977. Effusion rate and rheology of lunar lavas. Philos. Trans. R. Soc. Lond. A 285, 227–234.
Ishibashi, H., 2009. Non-Newtonian behaviour of plagioclase-bearing basaltic magma: subliquidus viscosity measurement of the 1707 basalt of Fuji volcano, Japan. J. Volcanol. Geotherm. Res. 181, 78–88.
Ishihara, K., Iguchi, M., Kamo, K., 1992. Numerical simulation of lava flows on some volcanoes in Japan. In: Fink, J.H. (Ed.), Lava Flows and Domes: Emplacement Mechanisms and Hazard Implications. Springer-Verlag, Berlin, pp. 174–207.
Iverson, R.M., 1992. Lava domes modelled as brittle shells that enclose pressurized magma, with application to Mount St. Helens. In: Fink, J.H. (Ed.), Lava Flows and Domes: Emplacement Mechanisms and Hazard Implications. Springer-Verlag, Berlin, pp. 47–69.
Kelfoun, K., Vallejo-Vargas, S., 2015. VolcFlow capabilities and potential development for the simulation of lava flows. In: Harris, A.J.L., De Groeve, T., Garel, F., Carn, S.A. (Eds.), Detecting, Modelling and Responding to Effusive Eruptions. Geological Society, London, Special Publications 426. (http://doi.org/10.1144/SP426.8).
Kerr, R.C., Lyman, A.W., 2007. Importance of surface crust strength during the flow of the 1988–1990 andesite lava of Lonquimay Volcano, Chile. J. Geophys. Res. 112, B03209. http://dx.doi.org/10.1029/2006JB004522.
Kerr, R.C., Griffiths, R.W., Cashman, K.V., 2006. Formation of channelized lava flows on an unconfined slope. J. Geophys. Res. 11, B10206. http://dx.doi.org/10.1029/2005JB004225.
Lipman, P.W., Banks, N.G., 1987. Aa flow dynamics, Mauna Loa. In: Decker, W., Wright, T.L., Stauffer, P.H. (Eds.), Volcanism in Hawaii. US Geol. Surv. Prof. Pap. 1350, pp. 1527–1567.
Lyman, A.W., Kerr, R.C., 2006. Effect of surface solidification on the emplacement of lava flows on a slope. J. Geophys. Res. 111, B05206.
Moitra, P., Gonnermann, H.M., 2015. Effects of crystal shape- and size-modality on magma rheology. Geochem. Geophys. Geosyst. 16, 1–26. http://dx.doi.org/10.1002/2014GC005554.
Moreno, H., Clavero, J., 2006. Geología del área del volcán Villarrica, Regiones de la Araucanía y de los Lagos. Servicio Nacional de Geología y Minería, Carta Geológica de Chile, Serie Geología Básica, 98,1 mapa escala 1:50.000, Santiago (in spanish)
Moreno, H., Gardeweg, M., 1989. La erupción reciente en el complejo volcánico Lonquimay (Diciembre 1988-) Andes del Sur. Rev. Geol. Chile 16, 93–117.
Morgado, E., Parada, M.A., Contreras, C., Castruccio, A., Gutiérrez, F., McGee, L.E., 2015. Contrasting records from mantle to surface of Holocene lavas of two nearby arc volcanic complexes: Caburgua-Huelemolle Small Eruptive Centers and Villarrica Volcano, Southern Chile. J. Volcanol. Geotherm. Res. 306, 1–16. http://dx.doi.org/10.1016/j.jvolgeores.2015.09.023.
Mueller, S., Llewellin, E.W., Mader, H.M., 2009. The rheology of suspensions of solid particles. Proc. R. Soc. 466, 1201–1228.
Naranjo, J.A., Sparks, R.S.J., Stasiuk, M.V., Moreno, H., Ablay, G.J., 1992. Morphological, structural and textural variations in the 1988–1990 andesite lava of Lonquimay Volcano. Chile. Geol. Mag. 129, 657–678.
Pinkerton, H., Norton, G.E., 1995. Rheological properties of basaltic lavas at sub-liquidus temperatures: laboratory and field measurements on lavas from Mount Etna. J. Volcanol. Geotherm. Res. 68, 307–323.
Pinkerton, H., Sparks, R.S.J., 1978. Field measurements of the rheology of lava. Nature 276, 383–385.
Pinkerton, H., Wilson, L., 1994. Factors controlling the lengths of channel-fed lava flows. Bull. Volcanol. 56, 108–120.
Proietti, C., Coltelli, M., Marsella, M., Fujita, E., 2009. A quantitative approach for evaluating lava flow simulation reliability: LavaSIM code applied to the 2001 Etna eruption. Geochem. Geophys. Geosyst. 10, Q09003. http://dx.doi.org/10.1029/2009GC002426.
Putirka, K., 2008. Thermometers and barometers for volcanic systems. Rev. Mineral. Geochem. 69, 61–120.
Ryerson, F.J., Weed, H.C., Piwinskii, A.J., 1988. Rheology of subliquidus magmas 1. Picritic compositions. J. Geophys. Res. 93, 3421–3436.
Saar, M., Manga, M., Cashman, K.V., Fremouw, S., 2001. Numerical models of the onset of yield strength in crystal-melt suspensions. Earth Planet. Sci. Lett. 187, 367–379.
Takagi, D., Huppert, H.E., 2010. Initial advance of long lava flows in open channels. J. Volcanol. Geotherm. Res. 195, 121–126.
Vicari, A., Ciraudo, A., Del Negro, C., Herault, A., Fortuna, L., 2009. Lava flow simulations using discharge rates from thermal infrared satellite imagery during the 2006 Etna eruption. Nat. Hazards 50, 539–550.
Vona, A., Romano, C., Dingwell, D.B., Giordano, D., 2011. The rheology of crystal-bearing basaltic magmas from Stromboli and Etna. Geochim. Cosmochim. Acta 75, 3214–3236.
Wadge, G., 1981. The variation of magma discharge during basaltic eruptions. J. Volcanol. Geotherm. Res. 11, 139–168.
Wadge, G., Young, P., McKendrick, I., 1994. Mapping lava flow hazards using computer simulation. J. Geophys. Res. 99, 489–504.
Walker, G.P.L., 1972. Compound and simple lava flows and flood basalts. Bull. Volcanol. 35, 579–590.
Wilson, L., 1993. Mecanismos eruptivos. In: Martí, J., Araña, V. (Eds.), La volcanología actual. Consejo Superior de Investigaciones Científicas, Madrid, pp. 45–97 (in spanish).